HHS Public Access

Author manuscript

Annu Rev Anal Chem (Palo Alto Calif). Author manuscript; available in PMC 2026 May 27.

Published in final edited form as:

Annu Rev Anal Chem (Palo Alto Calif). 2026 May ; 19(1): 95–120. doi:10.1146/annurev-anchem-101724-105925.

Single-Cell Protein Assays in Context: From 2D to 3D and In Situ Analysis

Jocelyn S. Baker[*],

Neica I. Joseph[*],

Alison Lao[*],

Julea Vlassakis

Department of Bioengineering, Rice University, Houston, Texas, USA;

Abstract

Single-cell proteomics (scP) is a crucial complement to transcriptomics, offering deeper insight into cellular heterogeneity, disease mechanisms, and therapeutic vulnerabilities in samples such as 2D cell culture, 3D models, and patient tissue. While transcriptomics enables high-throughput gene expression characterization, RNA levels frequently do not correlate with protein levels even in the same cell. Furthermore, protein isoforms, posttranslational modifications, and complexes are missed by transcriptomic analyses. This review explores modern scP technologies, including flow and mass cytometry, single-cell mass spectrometry, immunohistochemistry, cyclic imaging, and imaging mass cytometry applied to both dissociated and spatially preserved samples. We emphasize applying these techniques to organ-on-a-chip, organoids, spheroids, and intact tissues, highlighting advances in spatial resolution and multiplexing. We also discuss the trade-offs between throughput, spatial fidelity, and protein selectivity across platforms. Finally, we identify key measurement gaps, suggesting future directions toward spatially resolved scP clinical translation.

Keywords

single-cell proteomics; spatial proteomics; 3D tissue models; cytometry; sample preparation; imaging mass spectrometry

ylassakis@rice.edu .

[*]These authors contributed equally to this article

The *Annual Review of Analytical Chemistry* is online at anchem.annualreviews.org

DISCLOSURE STATEMENT

The authors are not aware of any affiliations, memberships, funding, or financial holdings that might be perceived as affecting the objectivity of this review.

INTRODUCTION

Over the past two decades, studying cell populations with greater detail to identify rare populations has become imperative to understanding complex biology. It is now well-recognized that many diseases are highly heterogeneous and that small subpopulations of cells can significantly influence patient outcomes. Since the first instance of single-cell-level RNA measurements in the 1990s (1, 2) and full-fledged single-cell transcriptomics in the late 2000s (3), elucidating human biology at a single-cell level has become recognized as a requirement for advancing knowledge of genetic conditions, cancers, and other diseases that still plague patients despite treatment advances.

While transcriptomics approaches have led to incredible insight into diseases and biological processes, documenting the transcriptome gives researchers only partial insight into how pathologies impact cells. Transcriptomics fails to detect certain disease biomarkers because of its inability to document posttranslational modifications (PTMs) and protein complexing dynamics, two cellular characteristics that are functional in disease targeting and potential druggability. Protein isoforms have different functions in diseased cells and may also not be detected by transcriptomics techniques, hindering the applicability of transcriptomics to research some pathologies (4). Studies integrating proteomics and transcriptomics reveal poor correlations between mRNA and protein levels in single cells, further demonstrating the value of studying single-cell proteomes (5, 6).

Multiple well-established techniques, including immunohistochemistry (IHC), immunocytochemistry (ICC), and flow cytometry (FC), can be considered single-cell proteomics (scP) techniques. However, modern scP techniques require higher throughput, sensitivity, selectivity, and multiplexing compared to traditional ICC and FC to fully delve into complex diseases and biological processes, especially in attempts to detect rare cell subpopulations (7) (Figure 1). Multiple cutting-edge scP techniques have been developed in research labs through assay and technology advancements, but such techniques have only recently become used in clinical settings. In this review, we cover the latest advances in scP techniques such as multiplexed FC, ICC/IHC, and single-cell mass spectrometry (scMS) and their application to three-dimensional (3D) models and tissue samples. The review is organized on the basis of techniques that do not preserve spatial information, such as cell-to-cell contact or location in tissues, versus techniques that do (Figure 2). We highlight the advantages and disadvantages of techniques in application to various samples and measurement gaps that serve as opportunities for innovation.

SINGLE-CELL PROTEIN TECHNIQUES THAT DO NOT PRESERVE SPATIAL CONTEXT

Many proteomics techniques have emerged to study heterogeneous cell populations on a single-cell level. Typically, these techniques involve isolating cells from a large population in suspension through microfluidics, geometric trapping, or other creative sample preparation methods before processing with various analytical methods. This section highlights several scP techniques that have emerged as high-throughput workhorses but are not spatially conservative (Table 1). Some methods are included in Table 1 to give

readers a complete view of the current scP landscape, but they are not discussed further due to significant limitations in throughput (8, 9). To meaningfully apply scP techniques to biological systems, high throughput is a necessity, along with high specificity and sensitivity in protein detection (Figure 1). Most techniques in Table 1 were developed with cells cultured in 2D environments, but progress is being made in adapting techniques for studying 3D systems or clinically relevant tissue samples, as discussed below.

Unlike 2D culture models, 3D models more accurately recapitulate key aspects of in vivo biology, including spatial architecture, cell–cell interactions, and gradients of nutrients and oxygen (10). These models include spheroids, patient-derived organoids, hydrogel scaffolds, and organ-on-a-chip platforms (Figure 2). However, cellular heterogeneity and cell-state dynamics in 3D models pose analytical challenges, particularly in achieving single-cell resolution. To address this, researchers are shifting away from bulk analysis approaches, which often obscure rare cell populations and spatially localized phenomena, toward developing single-cell analysis techniques compatible with 3D systems such as tumor microenvironment (TME) models. Such single-cell omic platforms have enabled precise dissection of tumor subpopulations, cell–cell communication, and phenotypic responses within spatially structured microenvironments (10). In this section, we also evaluate the applicability of scP techniques to dissociated 3D models and associated challenges.

FLOW CYTOMETRY AND MASS CYTOMETRY

FC is a widely used and well-documented high-throughput single-cell analysis technique. After cells are fluorescently labeled for markers of interest, a single-cell stream is generated to activate fluorescent labels with a laser and to optionally sort cells in a process termed fluorescence-activated cell sorting (FACS). FACS has been combined with cell barcoding to multiplex single-cell protein detection, making it a powerful and widely accepted single-cell analysis technique. FC is readily incorporated into cell biology, translational research, and clinical workflows. FACS has been used to study signaling pathways, to discover disease biomarkers, and to investigate pharmacodynamics (23). However, FC remains constrained by off-target antibody binding, batch-to-batch variability, and restricted multiplexing capacity due to its reliance on immunofluorescence. Addressing these issues requires careful antibody panel development and validation (24). Use of multiple antibodies specific to different epitopes on the same protein of interest (25) or proximity-ligation assay (PLA) can enhance specificity. Still, such techniques have challenges, including false complex detection with PLA (26, 27). Amplifying signals using rolling circle amplification can improve assay sensitivity (28, 29). However, multiplexing is still a bottleneck to FC’s application to complex, heterogeneous samples. Groups have made technological advancements in efforts to overcome these hindrances.

To advance FC’s sensitivity and specificity while maintaining high throughput, groups have developed microfluidic devices to combine FC with additional analysis methods like high-resolution microscopy. Unique microchip designs have been produced by the Sun and Wang groups (30, 31) to create constricted flow channels or uniform optical fields for imaging. This allows for continuous sample flow and creation of calibration curves to more accurately quantify absolute protein levels, thus improving the arbitrary output of traditional FC, in

which cells are identified as target positive or negative or relative protein concentration is reported. Furthermore, the Jia lab has shown the ability to combine high-resolution imaging with FC on a microfluidic device with improved 3D spatial resolution and throughput compared to past imaging FC (IFC) setups (32). The Jia lab's IFC technology detects protein abundance and gains intracellular protein localization information. Multiple commercially available IFCs have become available in recent years; however, they lack the spatial/subcellular resolution achieved above. Commercially available imaging flow cytometer systems such as Cytek Amnis (Cytek Biosciences) and BD FACSDiscover™ (BD Biosciences) make the general technique of IFC more accessible to clinical settings lacking the expertise to fabricate microfluidic devices.

Another approach to overcoming multiplexing limitations of fluorescence-based detection is using antibodies conjugated to heavy metal isotopes, as in CyTOF® (cytometry by time of flight) (Figure 3a). Standard multilaser flow cytometers can measure ~30 parameters but require complex spectral compensation and carefully optimized antibody panels. For example, Liechti & Roederer (33) developed a 28-color FC panel to analyze multiple parameters in peripheral blood monoclonal cells (PBMCs)—a process that required careful development and optimization. In contrast, CyTOF enables quantification of ~60 protein markers/cell with minimal signal overlap and no need for spectral compensation. Detection is achieved via mass spectrometry (MS), thereby bypassing the optical limitations of fluorescence.

FLOW CYTOMETRY– AND MASS CYTOMETRY–BASED PROTEOMIC PROFILING OF DISSOCIATED 3D SAMPLES

FC has been applied to dissociated 3D tumor models to provide insights into cellular responses and heterogeneity. Patra et al. (36) used FC to assess size-dependent drug responses in HepG2 hepatocellular carcinoma spheroids, finding enhanced drug resistance in larger spheroids. This work highlights how 3D culture contexts influence therapeutic outcomes, revealing behaviors not seen in 2D models. Similarly, de Villiers & Du Plessis (37) validated FC for assessing apoptosis in melanoma cells embedded in 3D bioprinted alginate–gelatin hydrogel scaffolds, confirming the compatibility of FC with enzymatically degelated hydrogel scaffolds for analysis of cell viability. Grässer et al. (38) further demonstrated FC's reliability in quantifying cellular composition in complex 3D spheroids, including human dermal fibroblasts and microvascular endothelial cells, optimizing enzymatic dissociation for monoculture and coculture spheroids and showing high cell recovery and viability post-dissociation.

FC can quantify immune cytotoxicity and cell behavior in 3D cocultures. Zhou et al. (39) used FC to predict patient-specific immune checkpoint inhibitor benefits in patient-derived cholangiocarcinoma organoids cocultured with T cells or PBMCs. Mcbain et al. (40) developed two advanced FC workflows to study T cell infiltration and immune-mediated tumor killing in 3D tumor spheroid cocultures. They quantified T cell activation phenotypes in infiltrated versus non-infiltrated T cells and assessed tumor killing dynamics, revealing temporal progression in T cell activation and exhaustion. $CD3^+$ T cell infiltration was

comparable in breast (617 ± 97) and ovarian (567 ± 105) spheroids but reduced in lung cancer (282 ± 41) spheroids. Beyond tumor models, Thomas et al. (41) developed CelltypeR, an FC-based pipeline with a 13-antibody panel and computational tools, to identify and quantify brain cell types in human induced pluripotent stem cell (iPSC)-derived midbrain organoids. This allowed them to track cell type composition and heterogeneity across time and iPSC lines.

Although CyTOF emerged recently, groups have also demonstrated its technological applications to 3D in vitro models. Qin et al. (42) modified the CyTOF workflow to analyze PTM signaling networks in healthy and colorectal cancer organoids. They developed a 28-antibody panel and a custom barcoding strategy for multiplexing, enabling the profiling of more than a million cells. Sufi et al. (43) used CyTOF with a 35-plex antibody panel to profile millions of cells from colorectal cancer organoids cocultured with stromal and immune cells. Their work provided high-dimensional proteomics maps of the TME, demonstrating CyTOF's ability to capture dynamic cell states and bidirectional cell signaling (43). Rosenbluth et al. (44) developed a 38-metal-tagged antibody panel for CyTOF to identify and quantify epithelial subtypes in patient-derived mammary organoids, including patients with inherited cancer mutations. Their analysis both revealed that organoid cultures retained major mammary epithelial lineages and identified increased luminal progenitor cells in BRCA1 mutation carriers, consistent with known cancer risk.

FC- and mass cytometry (MC)-based platforms offer relatively high-throughput tools for analysis of TME models. However, both methods require complete enzymatic dissociation of spheroids and organoids into single-cell suspensions, resulting in loss of spatial context and potential biases introduced during tissue digestion (45–47). Workflows may also involve fixation and permeabilization steps, particularly for intracellular or phospho-epitope profiling, which can impact antigen accessibility (48). Inadequate epitope preservation can reduce sensitivity or generate false negatives, resulting in inconsistent marker detection across sample types. Furthermore, substantial sample loss can occur during processing. Sample loss is problematic when working with low-input samples, such as small or rare organoids, where cell numbers could fall below the detection threshold for reliable quantification. CyTOF further requires well-validated metal-conjugated antibodies, and the instrumentation is costly, restricting accessibility. Despite these limitations, FC and MC remain widely adopted and scalable platforms for scP analyses of 3D models.

SINGLE-CELL IMMUNOBLOTTING

While FC has recently been used to make highly sensitive measurements at high throughput, the technique has limited selectivity for protein isoforms or complexes, except for PLA combined with IFC (49–51). However, protein complex detection assays such as PLA are limited to detecting dimeric complexes, despite many protein complexes having more than two subunits (52). Additionally, proximity-based detection approaches can falsely identify complexes, possibly providing misleading data (53). On a bulk scale, isoforms and protein complexes are detected with denaturing or native western blotting (WB). WB involves lysing thousands of cells, electrophoretically separating proteins in a polyacrylamide gel (PAG), and transferring proteins to a membrane for probing. WB techniques have been

adapted and miniaturized to develop single-cell immunoblotting assays (35, 54–56) (Figure 1b). These techniques employ microwells to isolate single cells for electrophoretic protein separation and utilize fluorescent probes for protein detection. Single-cell WB (scWB) entails gravity settling cells in microwells imprinted in a PAG, cell lysis, electrophoresis, UV photoimmobilization, and in-gel immunofluorescence probing. The Herr lab, which originated the scWB workflow, has shown the capacity to serially probe, image, and then strip and reprobe proteins captured in the PAG multiple times to detect approximately two dozen unique proteins/isoforms for hundreds to thousands of single cells per assay (17, 35, 54). scWB detects proteins with more than ~27,000 protein copies per cell, or approximately the top half of the mammalian proteome when one is considering copy numbers (35).

Work in multiple labs has addressed single-cell immunoblotting throughput, selectivity, and limitations of detection hindrances. The Herr lab (57) demonstrated electrophoretic separation of cellular lysates in the *z*-plane to increase sample density and throughput per device, differing from lateral/*x*–*y*-plane separation in the original protocol. Vlassakis, Hansen, and colleagues (55) separated monomeric proteins from complexed and nuclear content by using serial buffer applications and a bidirectional separation space for each microwell. This technique allows for the selective, simultaneous detection of cytoskeletal protein complex levels in hundreds of cells, expanding beyond dimeric protein complex detection. Adaptations to scWB buffer chemistry and electrophoretic separations have the potential to continue advancing the selectivity and throughput of single-cell immunoblotting.

To address the sensitivity of scWB, the Hughes lab has shown improved antibody probing and enzymatic amplification of protein signal (58). The group transferred proteins from PAGs onto nitrocellulose membranes by diffusion for further probing and/or signal amplification, which allowed for a 520-fold limit of detection improvement. The group sees decreased accuracy in quantifying proteins with high sensitivity, as immunofluorescence signal intensity does not correlate well with protein abundance ($R^2 = 0.3$). Even with this trade-off, such amplification techniques have not been compatible with previous immunoblotting approaches, due to gel pore size limitations that hinder diffusion of bulky amplification/probing molecules. The Ding group has addressed pore size limitations in scWB by using a temperature-controlled hydrogel for single-cell protein separations (27). The modified PAG has a contracted pore size to constrain protein band diffusion during electrophoretic separation. During probing, the gel can be chilled to increase pore size for improved antibody penetration. The group demonstrates reduced band diffusion during protein separation and imaging at high temperature and a 16-fold enhancement in signal compared to conventional scWB immunoprobing due to probing with a larger pore size at low temperature. Such assay modifications improve scWB sensitivity while maintaining throughput.

Single-cell immunoblotting techniques have not been extensively applied to 3D or spatially conservative samples. The Herr lab has recently shown the capacity to study the impact of cell-to-cell interaction on ERK signaling in cancer cells with a technique termed *Contact*Blot by culturing single cells in microwells and then allowing them to divide before immunoblotting (59).scWB has also been applied to several cancer cell lines and patient samples to gain insight into protein isoform presence and dynamics (54, 60). There

is excellent potential for single-cell immunoblotting techniques to be advanced for 3D applications to extend their insight to additional in vivo–relevant models.

SINGLE-CELL MASS SPECTROMETRY

MS is a robust platform that has advanced many fields, particularly cell metabolism and, very recently, scP. scMS can detect many more protein targets than can the assays discussed above. With creative sample preparation techniques, single-cell content can be labeled or remain isolated for scMS. However, absorptive loss or incomplete protein solubilization during sample preparation can significantly impact the robustness of single-cell data acquired with MS, and the following approaches aim to address such concerns.

NanoPOTS, developed in the Kelly lab, is a chip-based platform allowing for scMS preparation in a single-cell nanodroplet (21). A nanoscale liquid handling system delivers cells and then liquid chromatography–MS (LC-MS) reagents to microfabricated pedestals, minimizing liquid contact with the reaction vessel/space and adsorptive loss. The processed single-cell samples are collected in a fused silica capillary and sealed for LC-MS analysis. Due to the ultralow volumes, the Kelly group enhanced LC-MS sensitivity by using smaller columns and a (at the time) state-of-the-art mass spectrometer. NanoPOTS prep allowed for the detection of thousands of proteins per cell with a throughput of 10–100 mammalian cells. The group later introduced tandem-mass tags (TMTs) to single-cell droplets to increase sample density in a modified platform, NanoPOTS 2 (62).

To reduce sample loss and manual handling, recent scMS workflows use automated liquid handlers with advanced MS systems, achieving detection of thousands of proteins from ~120 cells/day (63). However, specialized equipment is extremely expensive, and limited throughput remains a bottleneck for truly impactful application of MS. To address this, multiple groups have reported microfluidic chips for LC-MS or data-independent acquisition MS (DIA-MS) sample preparation, reporting further automation, smaller sample volumes, and slightly higher throughput in some cases (64, 65). Improvements in sample detection and data processing are also critical for scMS sensitivity, throughput, and accessibility.

The Mann group achieved improved scMS sensitivity by isolating single cells via FACS for direct injection into MS instrumentation optimized for low-abundance ion detection (66). They later adapted the workflow to DIA-MS (67) (Figure 4a), which fragments all ions within predefined m/z windows and avoids reliance on ion intensity for precursor selection. This addresses a major limitation of conventional data-dependent methods, where low-abundance peptides in single cells often fail to trigger MS/MS scans (68). As a result, DIA-MS is especially well suited for the low protein content of single cells. The group combined this approach with dimethyl labeling, automated sample preparation, and a reference channel, which together enhanced both sensitivity and throughput (67).

Similar to NanoPOTS 2, SCoPE-MS relies on unique isobaric labels (TMTs) to identify single-cell proteome signatures when multiple single-cell samples are combined with a carrier sample to maximize peptide identifications (22, 69). Slavov and colleagues (22) expanded on this workflow to introduce SCoPE2, which incorporates automated,

miniaturized sample preparation for increased throughput. SCoPE2 can quantify ~3,000 proteins/cell, resolving distinct cell types and phenotypic gradients during lineage differentiation. However, applications have largely been limited to suspension and 2D-cultured cells. Extending SCoPE2 and similar methods to dissociated 3D tumor models like organoids or tumor-on-a-chip systems could enable proteomics profiling in more physiologically relevant microenvironments.

MASS SPECTROMETRY–BASED SINGLE-CELL PROTEOMICS ANALYSES OF DISSOCIATED 3D SAMPLES

While scMS has seen major advancements in 2D analysis, progress has also been made in extending these capabilities to 3D models. Martins et al. (68) applied DIA-MS with a custom analysis pipeline (DiagnoMass) to profile dissociated single cells from iPSC-derived brain organoids modeling Rett syndrome. The group achieved high-sensitivity peptide detection and distinguished neuroprogenitor cells from healthy controls versus patient-derived samples. DiagnoMass identified 9,027 spectral clusters from 306,036 tandem mass spectra, demonstrating the capacity of DIA-MS to capture condition-specific proteomics signatures in organoid-based systems. scMS has also been employed to profile cell type–specific proteomes from human cerebral organoids, as Melliou & Diamandis (70) demonstrated. Organoids were enzymatically dissociated into single-cell suspensions, and neural progenitors and immature neurons were isolated with FACS for LC-MS analysis. The group noted that progenitor cells were enriched for proteins involved in DNA replication and cell cycle regulation, while the immature neurons showed protein enrichment for axon development and neuronal projection. Notably, protein-level and transcriptional-level differences were noted, highlighting the value of proteomics analysis. These studies demonstrated MS-based temporal and cell type–specific proteomics profiling of organoids.

In addition to neural organoids and developmental investigations, Wang et al. (71) performed a comprehensive proteomics analysis of patient-derived gastric cancer organoids to evaluate how different Matrigel dissociation methods affect downstream MS. While their study did not use single-cell resolution, their findings are directly relevant to single-cell workflows, as they addressed a key technical barrier: the interference of extracellular matrix components like Matrigel with protein identification and quantification. They found that enzymatic digestion with dispase yielded the highest peptide recovery, the greatest number of identified proteins, and the most accurate quantification when compared to dissociation with cell recovery solution and PBS-EDTA. These results highlight best practices for minimizing matrix-derived artifacts when studying 3D models with MS. Looking ahead, applying DIA-MS to dissociated cell 3D systems could enable detailed, cell type–specific proteomics profiling within the TME. The ability of DIA to capture deep proteome coverage from low-input samples makes it especially well suited for complex, multicellular 3D systems in which material is often limited.

Beyond single-cell resolution, recent studies have used Orbitrap MS platforms (e.g., LTQ Orbitrap or Orbitrap Fusion) to analyze intact organoids as ultrasmall tissues. In a notable study, Nezvedová et al. (72) developed a protocol to profile both proteins and lipids from

individual human cerebral organoids. Organoids harvested at different developmental stages were processed using a tailored pipeline that enabled quantification of cell type markers and glycosphingolipids. This workflow generated a detailed snapshot of each organoid's cellular composition and maturation state. However, this study did not reach single-cell resolution, and similar analyses have not yet been reported for tumor models. Extending these Orbitrap-based workflows to TME models could provide a bridge between bulk organoid-level analysis and scP in the context of cancer biology.

SINGLE-CELL PROTEIN TECHNIQUES THAT CONSERVE SPATIAL INFORMATION

Eukaryotic cells synthesize tens of thousands of different kinds of proteins, each of which has evolved to function optimally in specific cellular and subcellular localizations and colocalizations (73). These specific localizations assign proteins to one of the cell compartments that perform specific biological functions (74, 75). Determining these locations can be used as guides for designing drugs, as the tight regulation of protein subcellular localization plays an important role in cell physiology (76). A protein's localization is important for its interaction with other molecules, and mislocalization is directly associated with various diseases (77, 78). For example, in Ewing sarcoma, a pediatric bone cancer prevalent in adolescents and characterized by the chimeric protein EWSR1/FLI1 (77), low EWSR1 levels correspond with a significantly high incidence of abnormal spindles and mislocalization of Aurora B kinase (79, 80), misregulating chromosome segregation during mitosis and increasing tumorigenesis (81). In cystic fibrosis, a genetic, life-threatening disease that causes overactive sweat and mucous glands, the most common mutation, CFTR 1F508, causes retention of the protein in the endoplasmic reticulum (ER) (82, 83), resulting in ER stress, increased SERCA activity, and abnormal Ca^{2+} release into the cytoplasm (84) and thus leading to dysregulation in airway epithelial and immune cells and hyperinflammation (85).

The following techniques can be applied to 2D- or 3D-dissociated single cells as well as intact tissue samples to gain spatial information. Single-cell localization within a tissue, proximity to or interaction with other cells, and individual cell morphology can be critically important when one is studying pathologies such as cancer or using single-cell techniques for diagnostics and treatment planning. Additionally, spatial proteomics, especially in situ methods (86–90), can resolve dynamic, heterogeneous, and morphologically contextual protein distributions, providing high-resolution, clinically relevant insights that overcome limitations of computational techniques (91–94) and catalogs (https://v22.proteinatlas.org, https://www.uniprot.org).

Immunocytochemistry

ICC has been a staple technique for proteomics analysis for decades, especially in diagnostic settings. However, traditional ICC is limited in throughput capacity and the number of protein targets detectable per assay. To address these hindrances, ICC technology and technique advances, including the introduction of quenchable fluorescent probes (6, 11, 95–101), have been made, allowing for more multiplexing and improved microscopy/analysis

techniques that improve sensitivity and throughput. Further improvements in throughput have been demonstrated as groups use automation techniques. For example, similar to probe stripping in scWB assays, cyclic immunofluorescence (CycIF) or highly multiplexed tissue imaging involves multiple rounds of staining, imaging, and fluorescence quenching/bleaching to detect multiple proteins/samples, providing phenotype/protein distribution information in intact samples. This technique has not reproducibly reached single-cell-level analysis due to image segmentation limitations and still requires lengthy sample processing times, but automation can greatly reduce hands-on sample processing time. Laborious analysis is also becoming more frequently automated with programs such as CellProfiler (102), napari (103), and ilastik (104), making complicated analysis pipelines more accessible.

A fluorescent detection–based cyclic ICC system that has emerged within the past few years is the ChipCytometry system from Zellkraft (97, 105). ChipCytometry utilizes microfluidics to automate all probing, imaging, and fluorescence bleaching steps involved in CycIF of formalin-fixed samples. ChipCytometry greatly increases the multiplexing abilities of CycIF compared to previous approaches, such as Vectra, which lack automation and can introduce human error, leading to the detection of fewer targets before samples are compromised. Additionally, ChipCytometry workflow allows for sample storage for up to 2 years, which can be advantageous in both clinical and research settings. Fluorescence-based CycIF approaches can have high throughput with automation, and reagents are more affordable than other approaches, making them the ideal choice for clinical settings. However, techniques that do not rely on fluorescence have been shown to be more multiplexable. One example is the co-detection by indexing (CODEX) system (Figure 4b), which can detect upward of 50 targets (61, 106); CODEX is a successor of immunoPCR techniques (107, 108). CODEX uses antibodies conjugated to barcodes for highly specific detection of the target-specific barcodes using a dye-labeled reporter (fluorophore) to provide information on relative protein abundance measurements at a single-cell level. Other DNA-barcode approaches have been shown to achieve single-cell resolution and can be paired with RNA profiling (GeoMx DSP) or offer more sample-friendly and reproducible staining (Ultivue's InSituPlex), but at a greater cost.

Cyclic Imaging in 3D Samples

The adoption of cyclic imaging workflows for achieving consistent single-cell resolution across intact 3D platforms—such as organoids and spheroids—remains an evolving frontier, despite this approach being well-established for fixed 2D tissue sections. Reynolds et al. (109) applied CycIF to patient-derived glioblastoma organoids (live and fixed samples). They assessed nine total surface and intracellular proteins across three cycles in fixed samples and six surface markers over two cycles in live organoids by quenching fluorescent signals using bioorthogonal click chemistry. Results showed heterogeneous expression and spatial colocalization of glioblastoma markers, and viability assays confirmed that the cyclic process did not impair organoid health or gene expression.

Bhaumik et al.(110) applied CycIF to formalin-fixed paraffin-embedded (FFPE) sections of 3D spheroids derived from lung and colorectal cancer cell lines, enabling simultaneous

visualization of four biomarkers per cancer panel. Optimized fluorophore–antibody pairings and iterative staining rounds yielded clear, compartment-specific multiplex signals, with expression profiles that aligned with expected biology. Spectral unmixing and automated quantification preserved subcellular localization and enabled detection of nuclear coexpression events within intact 3D spheroid sections. The workflow demonstrated that cyclic imaging could effectively multiplex biomarker analysis in 3D cultures while maintaining spatial integrity across cellular compartments. Dinevska et al. (111) developed a multiplex IHC workflow using FFPE microarrays of glioblastoma spheroids and patient-derived organoids. Spheroids were cultured in Cultrex invasion matrix, fixed, and spatially preserved in HistoGel, allowing for simultaneous analysis of multiple treatments and conditions on a single slide. Cyclic staining with Opal six-plex fluorophores enabled iterative detection of phosphorylated signaling proteins within intact 3D architecture, revealing subcellular localization and coexpression patterns across cells interacting with the extracellular matrix.

Harter et al. (112) developed a donor-matched 3D organoid system to study on-target off-tumor toxicity from T cell–engaging bispecific antibodies (TCBs), engineered antibodies that redirect T cells to kill target-expressing cells. They cocultured patient-derived intestinal organoids and donor-matched colorectal tumoroids with PBMCs in extracellular matrix hydrogels, then treated them with TCBs targeting antigens to model immune-mediated damage observed in clinical trials. A seven-plex CycIF workflow was applied to FFPE sections, enabling visualization of epithelial cells, immune subsets, apoptosis, and antigen expression. This approach revealed intraepithelial infiltration of CD4+ and CD8+ T cells into organoids before apoptosis onset, along with greater immune infiltration and epithelial damage in healthy organoids than in tumoroids, despite lower target expression.

Tomovetal. (113) developed a multiplexed imaging workflow to profile cell identity and state in heterogeneous neural cultures derived from human iPSCs. Motor and cortical neuron spheroids were differentiated in suspension and then dissociated and plated for 2D imaging. Their cyclic technique, PRISM, enabled iterative staining of more than 10 protein markers per sample without requiring antibody stripping or compromising cellular morphology. A validated 12-marker panel distinguished neuronal, glial, and progenitor populations while preserving subcellular localization. This approach facilitated high-content, single-cell phenotyping of stem cell–derived cultures across multiple developmental stages.

Looking ahead, CycIF holds promise for high-resolution, multiplexed analysis of intact 3D cultures. Although currently optimized for thin slices, advances in imaging depth, probe penetration, and signal stability could extend the application of CycIF to whole organoids and spheroids (114,115). Integrating tissue clearing, improved antibody delivery, and light-sheet or confocal microscopy may enable dynamic, spatially resolved insights into cellular heterogeneity and treatment response within fully intact 3D models.

Imaging Mass Cytometry in 3D Samples

Imaging mass cytometry (IMC) is widely used to analyze tumor tissues, although its application to 3D models remains an emerging area. Flint et al. (116) employed IMC to profile single-cell protein expression in a 3D aggregoid model derived from epithelial lung

adenocarcinoma cells, designed to better mimic the TME. Cryosectioned aggregoids (~1 mm in diameter) were stained with metal-conjugated antibodies targeting key epithelial, proliferative, and hypoxia-associated proteins (18, 117). IMC was performed via laser ablation at 1-μm resolution, followed by time-of-flight mass spectrometry, enabling spatial segmentation and mapping of proliferative, hypoxic, and necrotic aggregoid zones. In a subsequent study, Flint (118) published a detailed workflow on standardized sample preparation, staining, imaging, and data alignment for multimodal MS imaging (MSI) applications.

While IMC has been widely demonstrated on tissue samples, its application to 3D models remains limited. Embedding and sectioning organoids followed by IMC could enable high-dimensional in situ proteomics profiles of models including TMEs. However, there are several barriers, including antibody penetration, spatial resolution (119), and imaging throughput and sensitivity in denser samples. Nonetheless, recent advances—including improved clearing protocols, signal amplification chemistries, and faster laser ablation systems—are actively addressing challenges. As IMC protocols continue to advance, the technique holds potential for single-cell-level proteomics analysis within 3D models.

Multiplexed Immunohistochemistry for In Situ Tissue Analyses

Above, we discuss CycIF techniques, including automated systems and applications of their technology to 3D samples. Here, we turn to multiplexed ICC/IHC for clinical investigations, including MS-based approaches. IMC (120) has been extensively applied to human tissues to map cellular phenotypes and microenvironmental organization at high dimensionality. Multiplexed ion beam imaging (MIBI) (121–123), commercialized by Ionpath, also enables spatially resolved protein detection in tissue sections, supporting potential clinical integration. While both of these techniques use metal-tagged antibodies for high-plex spatial proteomics, IMC employs laser ablation for faster acquisition, whereas MIBI uses an ion beam for more sensitive protein measurements (124). MIBI also shows improved signal retention across repeated scans, but at the cost of slower throughput (125).

While these methods offer significantly greater multiplexing capacity than fluorescence-based ICC/IHC, they come with trade-offs. Cell segmentation for single-cell analysis remains challenging, especially in densely packed tissues, and the lower sensitivity compared to immunofluorescence limits detection of low-abundance markers (97, 126). Laser spot sizes (~1 μm) limit subcellular resolution and contribute to long imaging times. While IHC slides can be archived, the sample ablation in IMC and MIBI is destructive to tissue sections. Finally, both platforms require highly specialized instrumentation, posing a significant cost and accessibility barrier. Despite these limitations, IMC and MIBI's ability to generate high-dimensional, spatially resolved proteomics data from tissues continues to make them powerful tools.

Giesen et al. (120) developed a high-resolution IMC workflow by combining CyTOF with IHC/ICC and laser ablation. Antibodies were labeled with rare-earth metal isotopes and applied to breast cancer tissue sections and adherent cell cultures. A laser ablation system scanned the tissue at 1-μm resolution, and the ablated material was analyzed by CyTOF to detect 32 targets. The resulting data were reconstructed into spatially resolved images,

and single-cell features were extracted computationally, allowing for the identification of distinct cell populations and signaling states within the TME. 3D spatial architecture can be identified by analysis of multiple adjacent slices of the intact breast tumors. This enabled the analysis of spatial gradients of marker expressions, including hypoxia toward the tumor core, and signaling interactions were observed at the tumor–stroma boundary.

Hosogane et al. (127) developed SABER-IMC, integrating IMC with DNA-barcoded signal amplification (immuno-SABER) to detect low-abundance proteins. They applied SABER-IMC to human melanoma and tonsil tissue and to a mixed cell pellet. The workflow involved conjugating antibodies with DNA bridge sequences, hybridizing them with DNA concatemers, and labeling with metal isotope–labeled imager strands for up to three rounds of amplification, boosting signal intensity up to 68-fold. This enabled simultaneous imaging of 38 markers in human melanoma tissue, including low-abundance immunomodulatory molecules, providing single-cell resolution within the preserved spatial architecture.

Kuett et al.(18) introduced a novel pipeline for 3D IMC by extending conventional IMC to serially sectioned FFPE tissue blocks derived from cylindrical breast carcinoma samples. They cut up to 152 consecutive sections, each stained with a panel of ~40 metal-tagged antibodies. The resulting images were reconstructed into 3D voxel models. Single-cell segmentation and clustering were performed, enabling spatially resolved phenotyping of thousands of cells and mapping of cellular neighborhoods and interaction networks. This 3D reconstruction visualized spatial gradients and tissue architecture, revealing features like microinvasive tumor protrusions and lymphovascular invasion events that are difficult to interpret from 2D sections alone.

Lin et al.(6) developed and applied tissue-based CycIF (t-CycIF) by applying sequential rounds of immunofluorescence staining, imaging, and fluorophore bleaching. Each cycle captured up to three protein markers and a nuclear dye, and the process is repeated to build up to 60-plex images from a single FFPE tissue section. t-CycIF was applied to a range of clinically relevant human samples, including tumors. With t-CycIF, 3D architecture was preserved for analysis of tumor–stroma boundaries, immune infiltration gradients, and microenvironment niches. In metastatic melanoma samples, the spatial distribution of immune checkpoint markers was mapped out, and immune-excluded versus immune-infiltrated regions were visualized.

EMERGING TECHNOLOGIES: IN SITU SPATIAL PROTEOMICS

Spatial proteomics techniques involve trade-offs between multiplexing capability, spatial resolution, data acquisition time, tissue coverage, and sensitivity (128,129). Highly multiplexed methods may sacrifice spatial resolution, while techniques that achieve single-cell or subcellular detail may detect fewer proteins, cover smaller areas, and mandate complex imaging and computational processing. Emerging in situ spatial proteomics technologies, including imaging MS-based techniques and intelligent image–based proteomics, aim to balance these criteria.

Mass Spectrometry–Based Approaches

MS can be used in in situ proteomics techniques to conserve spatial information of organoids and tissue samples. MSI enables label-free spatial analysis, identifying protein localization maps by acquiring a mass spectrum at each pixel from the tissue grid and converting these into corresponding m/z ratios that are identified and turned into spatial heat maps (130–133).

Various MSI techniques cover wide applications for analyzing spatial distributions of diverse biomolecules. In nanospray desorption electrospray ionization (nano-DESI), a solvent flows through a capillary over tissues at high voltage and extracts molecules into a liquid bridge transferred via ionizing electrospray to the MS to achieve a 10-μm spatial resolution (134, 135). The Laskin group (136) has improved this to a 7-μm resolution by optimizing probe design and section thickness to enhance the sensitivity and stability of protein signals, using nano-DESI for label-free proteoform mapping in mouse brain. This on-tissue, top-down approach identifies less commonly abundant endogenous proteoforms, such as myelin basic protein in cerebellar white matter and hemoglobin subunit alpha in blood vessels, and can perhaps help generate targeted therapies. This flexible method has also been applied to phospholipid analysis, enabling researchers to image and quantify 22 phosphatidylcholine species in seven different brain regions using simultaneous imaging and lipidomics shotgun-like quantification (135) and thereby advancing our knowledge of various biochemical pathways.

While nano-DESI excels in heterogeneous tissue section analysis, 3D imaging of solvent-cleared organs profiled by mass spectrometry (DISCO-MS) opens up the third dimension and integrates whole-organ clearing, deep learning–based image analysis, robotic extraction, and ultrasensitive MS (137, 138). Clearing renders organs transparent for imaging, and robotic extraction enables precise automated 3D sampling, achieving ultrahigh sensitivity compared to uncleared tissue samples. After end-to-end tissue imaging, DISCO-MS has revealed spatial immune heterogeneity in mouse bones and plaque heterogeneity in the human coronary artery (137) and has enabled the identification of isoforms and thousands of unique proteins while reporting proteins shared across respective regions and those that are up- and downregulated.

To improve resolution while maintaining throughput, tissue expansion MS imaging (TEMI) was developed (129, 139). By embedding tissues in hydrogels and denaturing them at high temperatures, they expand uniformly up to 10–20 times, allowing for high-resolution profiling of hundreds of analytes at single-cell resolution. ProteomEx, a TEMI-based method from the Piatkevich lab, enables spatial profiling of mammalian tissue at ~160-μm resolution using just 0.61 nL of sample and eightfold expansion (129), outperforming DISCO-MS and nano-DESI in true spatial granularity.

Another MS-based method, SPOT (spatial proteomics through on-site tissue protein labeling), enables spatially resolved profiling and the localization of proteins in their native environment via on-tissue TMT labeling. SPOT is compatible with frozen and FFPE tissues (140), has been applied to prostate cancer to profile thousands of peptides corresponding to hundreds of unique proteins, and is advantageous for identifying heterogeneity and global

proteomics changes associated with pathological states. Integrating machine learning–assisted tissue manipulation and processing could enhance SPOT's resolution to capture localized heterogeneity at the single-cell level.

Intelligent Image–Based In Situ Proteomics

While MS-based techniques can capture spatially localized molecular signals, a complementary class of approaches leverages high-resolution imaging, computational image segmentation, and integrative machine learning to offer streamlined, region-specific proteomics profiling at a higher spatial resolution and to capture heterogeneity within complex tissues.

Deep visual proteomics (DVP) integrates AI-based image analysis, single-nucleus or single-cell laser capture microdissection (LCM), and high-sensitivity MS for connecting images with single-cell-resolution protein abundance (141, 142). After segmenting tissue into regions of interest, histologically pure cells (typically hundreds to more than a thousand per experiment) are isolated via LCM for MS analysis (143, 144). At the Mann lab, DVP linked proteomics profiles to cell phenotypes in melanoma, revealing proteome changes during disease progression, such as mRNA splicing dysregulation and reduced interferon signaling (141). DVP has been used to phenotype across several disease stages in protein misfolding diseases, like α1-antitrypsin deficiency in human liver disease, identifying >20,000 precursors and >4,000 unique proteins from ~100 cells or 250–300 nuclei per region (142). Similarly, DVP has also been used to explore the tumor–immune microenvironment in colorectal cancer, exposing macrophage barriers inhibiting T cell infiltration and providing spatial insights into immunotherapy targets for personalized oncology (145). However, DVP remains limited by small sample cohorts and single-time-point data analysis, which cannot fully capture dynamic signaling interactions.

Sparse sampling strategy for spatial proteomics (S4P) addresses MS time constraints of whole-tissue slice–based proteomics (~8,000 h for 1 cm^2 at 100-μm resolution). It uses angled tissue strip sampling and computational reconstruction to map protein distributions within large samples at an ~500-μm resolution (146). In mouse brain, S4P has been leveraged to create a multilayer perceptron neural network framework, mapping 9,204 proteins at a 525-μm spatial resolution and achieving 15–20× faster MS times than gridding methods while maintaining regional proteome patterns. However, LCM-based collection in S4P causes adjacent tissue damage while cutting the target area and is currently limited to ~100-μm strips, while 3D spatial reconstruction requires at least eight slices spanning 80 μm along the *z*-axis to obtain the final spatial proteome profile, so further algorithmic refinement is needed to reduce sampling burden in sparse clinical settings.

Parallel-flow projection and transfer learning across omics data (PLATO) is another technique that integrates microfluidics and deep learning for high-resolution whole-tissue mapping (147). In this method, parallel-flow projections are created as first and third slices of tissue are digested on chip for LC-MS, while the middle slice is used for imaging or transcriptomics. PLATO employs transfer learning with the Flow2Spatial algorithm to reconstruct spatial expression patterns within the mouse cerebellum and intestinal villi, profiling ~3,000 protein groups at 2-μm resolution using only ~60 MS measurements.

Some disadvantages of PLATO are that it does not yet achieve single-cell resolution and necessitates higher-precision microfluidic channels to achieve a 10-μm resolution. Additionally, the sample workflow and slow speed of the MS instrument currently limit its ability to be used as a routine clinical diagnostic tool. It also cannot capture PTMs, which are important in understanding the functions and physicochemical properties of proteins (148).

CODEX can similarly provide spatial proteomics profiling information in tissues at a single-cell resolution in addition to its aforementioned use on 2D samples. By using a panel of 47 oligonucleotide-barcoded antibodies and iterative fluorescence labeling and imaging, CODEX has been used to help identify more than 28 unique cell types in human colon tissue, demonstrating its ability to resolve complex tissue architecture. CODEX is compatible with FFPE and fresh-frozen samples and integrates advanced bioinformatics tools for cell segmentation, normalization techniques, and unsupervised clustering algorithms to map cellular neighborhoods and to understand tissue-level immune dynamics (126). However, CODEX is not label free and is time consuming, and downstream analytical methods are needed to address noise in multiplexed imaging data to improve the signal-to-noise ratio.

FUTURE OUTLOOK FOR CLINICALLY INTEGRATED SPATIAL PROTEOMICS

While recent technological advancements in spatial proteomics have improved our ability to gather protein-level information from single cells, technical challenges still limit the potential of in situ proteomics. Across imaging and MS platforms summarized in Figure 5—including DVP, DISCO-MS, and TEMI—there remains a struggle to balance trade-offs like sensitivity, spatial resolution, speed, and throughput. Multiplexed imaging systems must manage fluorophore cross talk and photobleaching across cycles, while MS-based workflows often require time-consuming preparation to reduce protein loss. Standardizing data handling, segmentation, quantification, and optimizing instrumentation also remains difficult, especially as samples shift from dissociated cells to complex 3D tissues and clinical specimens. Robust validation and optimization are still needed for clinical use. For example, the PLATO workflow (147) is not yet compatible with fast-paced settings. The need for multiple tissue samples for S4P (146) and its potential for tissue damage may also limit its use with sparse specimens. Finally, the diversity of AI image segmentation algorithms and lack of standardized workflows across technologies may hinder accessibility for noncomputational scientists (149).

Despite these challenges, the potential of intelligent spatial proteomics is vast. Tools combining imaging, machine learning, and proteomics quantification are mapping protein distributions in intact tissues, revealing tumor-immune structures, and enhancing analysis in 2D and 3D models. As sensitivity and automation improve, these methods will become more scalable, preserving spatial context often lost in dissociated workflows and enabling future diagnostic and therapeutic applications.

ACKNOWLEDGMENTS

The authors would like to acknowledge their funding sources, including Cancer Prevention and Research Institute of Texas (CPRIT) grant RR210028 and the National Institute of Health (NIH) Director's New Innovator Award project number 1DP2CA290802-01.

LITERATURE CITED

1. Lambolez B, Audinat E, Bochet P, Crépel F, Rossier J. 1992. AMPA receptor subunits expressed by single Purkinje cells. Neuron 9(2):247–58 [PubMed: 1323310]
2. Eberwine J, Yeh H, Miyashiro K, Cao Y, Nair S, et al. 1992. Analysis of gene expression in single live neurons. PNAS 89(7):3010–14 [PubMed: 1557406]
3. Tang F, Barbacioru C, Wang Y, Nordman E, Lee C, et al. 2009. mRNA-Seq whole-transcriptome analysis of a single cell. Nat. Methods 6(5):377–82 [PubMed: 19349980]
4. Zhang Z,Pal S,Bi Y,Tchou J,Davuluri RV.2013.Isoform level expression profiles provide better cancer signatures than gene level expression profiles. Genome Med. 5(4):33 [PubMed: 23594586]
5. Darmanis S, Gallant CJ, Marinescu VD, Niklasson M, Segerman A, et al. 2016. Simultaneous multiplexed measurement of RNA and proteins in single cells. Cell Rep. 14(2):380–89 [PubMed: 26748716]
6. Lin J-R, Fallahi-Sichani M, Sorger PK. 2015. Highly multiplexed imaging of single cells using a high-throughput cyclic immunofluorescence method. Nat. Commun 6:8390 [PubMed: 26399630]
7. Davis A, Gao R, Navin NE. 2019. SCOPIT: sample size calculations for single-cell sequencing experiments. BMC Bioinformat. 20(1):566
8. Levy E, Slavov N. 2018. Single cell protein analysis for systems biology. Essays Biochem. 62(4):595–605 [PubMed: 30072488]
9. Xie H, Ding X. 2022. The intriguing landscape of single-cell protein analysis. Adv. Sci 9(12):2105932
10. Landon-Brace N, Li NT, McGuigan AP. 2023. Exploring new dimensions of tumor heterogeneity: the application of single cell analysis to organoid-based 3D in vitro models. Adv. Healthc. Mater 12(26):2300903 [PubMed: 37589373]
11. Klaesson A, Grannas K, Ebai T, Heldin J, Koos B, et al. 2018. Improved efficiency of in situ protein analysis by proximity ligation using UnFold probes. Sci. Rep 8(1):5400 [PubMed: 29599435]
12. Yang L, Wang Z, Deng Y, Li Y, Wei W, Shi Q. 2016. Single-cell, multiplexed protein detection of rare tumor cells based on a beads-on-barcode antibody microarray. Anal. Chem 88(22):11077–83 [PubMed: 27644430]
13. Chen Z, Lu Y, Zhang K, Xiao Y, Lu J, Fan R. 2019. Multiplexed, sequential secretion analysis of the same single cells reveals distinct effector response dynamics dependent on the initial basal state. Adv. Sci 6(9):1801361
14. Xue Q, Bettini E, Paczkowski P, Ng C, Kaiser A, et al. 2017. Single-cell multiplexed cytokine profiling of CD19 CAR-T cells reveals a diverse landscape of polyfunctional antigen-specific response. J. Immunother. Cancer 5(1):85 [PubMed: 29157295]
15. Shen B, Pade LR, Choi SB, Muñoz-LLancao P, Manzini MC, Nemes P. 2022. Capillary electrophoresis mass spectrometry for scalable single-cell proteomics. Front. Chem 10:863979 [PubMed: 35464213]
16. DeNiro G, Que K, Fujimoto T, Koo SM, Schneider B, et al. 2024. OMIP-105: a 30-color full-spectrum flow cytometry panel to characterize the immune cell landscape in spleen and tumor within a syngeneic MC-38 murine colon carcinoma model. Cytometry A 105(9):659–65 [PubMed: 39107997]
17. Gopal A, Herr AE. 2019. Multiplexed in-gel microfluidic immunoassays: characterizing protein target loss during reprobing of benzophenone-modified hydrogels. Sci. Rep 9(1):15389 [PubMed: 31659305]
18. Kuett L, Catena R, Özcan A, Plüss A, Cancer Grand Challenges IMAXT Consortium, et al. 2021. Three-dimensional imaging mass cytometry for highly multiplexed molecular and

cellular mapping of tissues and the tumor microenvironment. Nat. Cancer 3(1):122–33 [PubMed: 35121992]

19. Bendall SC, Simonds EF, Qiu P, Amir ED, Krutzik PO, et al. 2011. Single-cell mass cytometry of differential immune and drug responses across a human hematopoietic continuum. Science 332(6030):687–96 [PubMed: 21551058]
20. Budnik B, Levy E, Harmange G, Slavov N. 2018. SCoPE-MS: Mass spectrometry of single mammalian cells quantifies proteome heterogeneity during cell differentiation. Genome Biol. 19(1):161 [PubMed: 30343672]
21. Zhu Y, Piehowski PD, Zhao R, Chen J, Shen Y, et al. 2018. Nanodroplet processing platform for deep and quantitative proteome profiling of 10–100 mammalian cells. Nat. Commun 9:882 [PubMed: 29491378]
22. Specht H, Emmott E, Petelski AA, Huffman RG, Perlman DH, et al. 2021. Single-cell proteomic and transcriptomic analysis of macrophage heterogeneity using SCoPE2. Genome Biol. 22(1):50 [PubMed: 33504367]
23. Krutzik PO, Nolan GP. 2006. Fluorescent cell barcoding in flow cytometry allows high-throughput drug screening and signaling profiling. Nat. Methods 3(5):361–68 [PubMed: 16628206]
24. Uhlen M, Bandrowski A, Carr S, Edwards A, Ellenberg J, et al. 2016. A proposal for validation of antibodies. Nat. Methods 13(10):823–27 [PubMed: 27595404]
25. Kalina T, Lundsten K, Engel P. 2020. Relevance of antibody validation for flow cytometry. Cytometry A 97(2):126–36 [PubMed: 31577065]
26. Leuchowius K-J, Weibrecht I, Söderberg O. 2011. In situ proximity ligation assay for microscopy and flow cytometry. Curr. Protoc. Cytometry 56(1):9.36.1–15
27. Xie H, Guo W, Jiang H, Zhang T, Zhao L, et al. 2024. Photosensitive hydrogel with temperature-controlled reversible nano-apertures for single-cell protein analysis. Adv. Sci 11(19):2308569
28. Gusev Y, Sparkowski J, Raghunathan A, Ferguson H, Montano J, et al. 2001. Rolling circle amplification. Am. J. Pathol 159(1):63–69 [PubMed: 11438455]
29. Garafutdinov RR, Sakhabutdinova AR, Gilvanov AR, Chemeris AV.2021. Rolling circle amplification as a universal method for the analysis of a wide range of biological targets. Russ. J. Bioorg. Chem47(6):1172–89 [PubMed: 34931113]
30. Gao C, Zhang T, Wei Y, Liu Q, Ma L, et al. 2023. Development of a microfluidic flow cytometer with a uniform optical field (Uni-μFCM) enabling quantitative analysis of single-cell proteins and its applications in leukemia gating, tumor classification, and hierarchy of cancer stem cells. ACS Sens. 8(9):3498–509 [PubMed: 37602731]
31. Li X, Fan B, Liu L, Chen D, Cao S, et al. 2018. A microfluidic fluorescent flow cytometry capable of quantifying cell sizes and numbers of specific cytosolic proteins. Sci. Rep 8(1):14229 [PubMed: 30242168]
32. Hua X, Han K, Mandracchia B, Radmand A, Liu W, et al. 2024. Light-field flow cytometry for high-resolution, volumetric and multiparametric 3D single-cell analysis. Nat. Commun 15:1975 [PubMed: 38438356]
33. Liechti T, Roederer M. 2019. OMIP-060: 30-parameter flow cytometry panel to assess T cell effector functions and regulatory T cells. Cytometry A 95(11):1129–34 [PubMed: 31334913]
34. Tracey LJ, An Y, Justice MJ. 2021. CyTOF: an emerging technology for single-cell proteomics in the mouse. Curr. Protoc 1(4):e118 [PubMed: 33887117]
35. Hughes AJ, Spelke DP, Xu Z, Kang C-C, Schaffer DV, Herr AE. 2014. Single-cell western blotting. Nat. Methods 11(7):749–55 [PubMed: 24880876]
36. Patra B, Peng C-C, Liao W-H, Lee C-H, Tung Y-C. 2016. Drug testing and flow cytometry analysis on a large number of uniform sized tumor spheroids using a microfluidic device. Sci. Rep 6(1):21061 [PubMed: 26877244]
37. de Villiers M, Du Plessis LH. 2023. Flow cytometry as an analytical method of drug-induced apoptosis in 3D bioprinted melanoma cells. Biomed. Mater 18(4):045031
38. Grässer U, Bubel M, Sossong D, Oberringer M, Pohlemann T, Metzger W. 2018. Dissociation of mono- and co-culture spheroids into single cells for subsequent flow cytometric analysis. Ann. Anat 216:1–8 [PubMed: 29162481]

39. Zhou G, Lieshout R, van Tienderen GS, de Ruiter V, van Royen ME, et al. 2022. Modelling immune cytotoxicity for cholangiocarcinoma with tumour-derived organoids and effector T cells. Br. J. Cancer 127(4):649–60 [PubMed: 35597867]
40. Mcbain K, Oliver M, Bevan N, Szybut C. 2021. Quantifying T cell response in 3D tumor spheroids using advanced flow cytometry workflows. Appl. Note, Sartorius
41. Thomas RA, Sirois J, Li S, Gestin A, Deyab G, et al. 2024. CelltypeR: a flow cytometry pipeline to characterize single cells from brain organoids. iScience 27(9):110613 [PubMed: 39224516]
42. Qin X, Sufi J, Vlckova P, Kyriakidou P, Acton SE, et al. 2020. Cell-type-specific signaling networks in heterocellular organoids. Nat. Methods 17(3):335–42 [PubMed: 32066960]
43. Sufi J, Qin X, Rodriguez FC, Bu YJ, Vlckova P, et al. 2021. Multiplexed single-cell analysis of organoid signaling networks. Nat. Protoc 16(10):4897–918 [PubMed: 34497385]
44. Rosenbluth JM, Schackmann RCJ, Gray GK, Selfors LM, Li CM-C, et al. 2020. Organoid cultures from normal and cancer-prone human breast tissues preserve complex epithelial lineages. Nat. Commun 11:1711 [PubMed: 32249764]
45. Metzger W, Rösch B, Sossong D, Bubel M, Pohlemann T. 2021. Flow cytometric quantification of apoptotic and proliferating cells applying an improved method for dissociation of spheroids. Cell Biol. Int 45(8):1633–43 [PubMed: 33913594]
46. Fernandes NAR, Nascimento CR, Coletta RD, Rossa C Jr. 2025. A method for dissociation of oral cancer cell spheroids generated by magnetic 3D bioprinting. Cytotechnology 77(3):115 [PubMed: 40488212]
47. Herbig M, Tessmer K, Nötzel M, Nawaz AA, Santos-Ferreira T, et al. 2022. Label-free imaging flow cytometry for analysis and sorting of enzymatically dissociated tissues. Sci. Rep 12(1):963 [PubMed: 35046492]
48. Melan MA. 1995. Overview of cell fixation and permeabilization. In Immunocytochemical Methods and Protocols, ed. Javois LC, pp. 55–66. Humana Press
49. Andersen SS, Hvid M, Pedersen FS, Deleuran B. 2013. Proximity ligation assay combined with flow cytometry is a powerful tool for the detection of cytokine receptor dimerization. Cytokine 64(1):54–57 [PubMed: 23726671]
50. Krzeptowski W, Chudy P, Sokołowski G, Żukowska M, Kusienicka A, et al. 2021. Proximity ligation assay detection of protein–DNA interactions—is there a link between heme oxygenase-1 and G-quadruplexes? Antioxidants 10(1):94 [PubMed: 33445471]
51. Marcatti M, Jamison D, Fracassi A, Zhang W-R, Limon A, Taglialatela G. 2023. A method to study human synaptic protein-protein interactions by using flow cytometry coupled to proximity ligation assay (Syn-FlowPLA). J. Neurosci. Methods 396:109920 [PubMed: 37459899]
52. Giurgiu M, Reinhard J, Brauner B, Dunger-Kaltenbach I, Fobo G, et al. 2019. CORUM: the comprehensive resource of mammalian protein complexes—2019. Nucleic Acids Res. 47(D1):D559–63 [PubMed: 30357367]
53. Xia J, Phan HV, Vistain L, Chen M, Khan AA, Tay S. 2024. Computational prediction of protein interactions in single cells by proximity sequencing. PLOS Comput. Biol 20(3):e1011915 [PubMed: 38483861]
54. Kang C-C, Yamauchi KA, Vlassakis J, Sinkala E, Duncombe TA, Herr AE. 2016. Single cell–resolution western blotting. Nat. Protoc 11(8):1508–30 [PubMed: 27466711]
55. Vlassakis J, Hansen LL, Higuchi-Sanabria R, Zhou Y, Tsui CK, et al. 2021. Measuring expression heterogeneity of single-cell cytoskeletal protein complexes. Nat. Commun 12:4969 [PubMed: 34404787]
56. Tentori AM, Yamauchi KA, Herr AE. 2016. Detection of isoforms differing by a single charge unit in individual cells. Angew. Chem. Int. Ed 55(40):12431–35
57. Grist SM, Mourdoukoutas AP, Herr AE. 2020. 3D projection electrophoresis for single-cell immunoblotting. Nat. Commun 11:6237 [PubMed: 33277486]
58. Long MA, Benman W, Petrikas N, Bugaj LJ, Hughes AJ. 2023. Enhancing single-cell western blotting sensitivity using diffusive analyte blotting and antibody conjugate amplification. Anal. Chem 95:17894–902 [PubMed: 37974303]

59. Zhang Y, Naguro I, Ryuno H, Herr AE. 2024. *Contact*Blot: microfluidic control and measurement of the cell–cell contact state to assess contact-inhibited ERK signaling. Anal. Chem 96(38):15330–37 [PubMed: 39254112]
60. Sinkala E, Sollier-Christen E, Renier C, Rosàs-Canyelles E, Che J, et al. 2017. Profiling protein expression in circulating tumour cells using microfluidic western blotting. Nat. Commun 8:14622 [PubMed: 28332571]
61. Kennedy-Darling J, Bhate SS, Hickey JW, Black S, Barlow GL, et al. 2021. Highly multiplexed tissue imaging using repeated oligonucleotide exchange reaction. Eur. J. Immunol 51(5):1262–77 [PubMed: 33548142]
62. Woo J, Williams SM, Markillie LM, Feng S, Tsai C-F, et al. 2021. High-throughput and high-efficiency sample preparation for single-cell proteomics using a nested nanowell chip. Nat. Commun 12:6246 [PubMed: 34716329]
63. Ye Z, Sabatier P, Van Der Hoeven L, Lechner MY, Phlairaharn T, et al. 2025. Enhanced sensitivity and scalability with a Chip-Tip workflow enables deep single-cell proteomics. Nat. Methods 22(3):499–509 [PubMed: 39820750]
64. Gebreyesus ST, Siyal AA, Kitata RB, Chen ES-W, Enkhbayar B, et al. 2022. Streamlined single-cell proteomics by an integrated microfluidic chip and data-independent acquisition mass spectrometry. Nat. Commun 13:37 [PubMed: 35013269]
65. Yang Z, Jin K, Chen Y, Liu Q, Chen H, et al. 2024. AM-DMF-SCP: integrated single-cell proteomics analysis on an active matrix digital microfluidic chip. JACS Au 4(5):1811–23 [PubMed: 38818059]
66. Brunner A-D, Thielert M, Vasilopoulou C, Ammar C, Coscia F, et al. 2022. Ultra-high sensitivity mass spectrometry quantifies single-cell proteome changes upon perturbation. Mol. Syst. Biol 18(3):e10798 [PubMed: 35226415]
67. Thielert M, Itang EC, Ammar C, Rosenberger FA, Bludau I, et al. 2023. Robust dimethyl-based multiplex-DIA doubles single-cell proteome depth via a reference channel. Mol. Syst. Biol 19(9):e11503 [PubMed: 37602975]
68. Martins AMA, Santos MDM, Camillo-Andrade AC, Leite AL, Souza JS, et al. 2024. Integrating DIA single-cell proteomics data with the DiagnoMass proteomic hub for biological insights. J. Am. Soc. Mass Spectrom 35(10):2308–14 [PubMed: 39258941]
69. Tsai C-F, Zhao R, Williams SM, Moore RJ, Schultz K, et al. 2020. An improved boosting to amplify signal with isobaric labeling (iBASIL) strategy for precise quantitative single-cell proteomics. Mol. Cell. Proteom 19(5):828–38
70. Melliou S, Diamandis P. 2022. Generation of cell-type-specific proteomes of neurodevelopment from human cerebral organoids. STAR Protoc. 3(4):101774 [PubMed: 36313540]
71. Wang M, Yu H, Zhang T, Cao L, Du Y, et al. 2022. In-depth comparison of matrigel dissolving methods on proteomic profiling of organoids. Mol. Cell. Proteom 21(1):100181
72. Nezvedová M, Jha D, Váňová T, Gadara D, Klímová H, et al. 2023. Single cerebral organoid mass spectrometry of cell-specific protein and glycosphingolipid traits. Anal. Chem 95(6):3160–67 [PubMed: 36724094]
73. Dönnes P, Höglund A. 2004. Predicting protein subcellular localization: past, present, and future. Genom. Proteom. Bioinformat 2(4):209–15
74. Zhang Y-H, Ding S, Chen L, Huang T, Cai Y-D. 2022. Subcellular localization prediction of human proteins using multifeature selection methods. Biomed. Res. Int 2022:3288527 [PubMed: 36132086]
75. Pan X, Li H, Zeng T, Li Z, Chen L, et al. 2021. Identification of protein subcellular localization with network and functional embeddings. Front. Genet 11:626500 [PubMed: 33584818]
76. Bauer NC, Doetsch PW, Corbett AH. 2015. Mechanisms regulating protein localization. Traffic 16(10):1039–61 [PubMed: 26172624]
77. Park S, Yang J-S, Shin Y-E, Park J, Jang SK, Kim S. 2011. Protein localization as a principal feature of the etiology and comorbidity of genetic diseases. Mol. Syst. Biol 7:494 [PubMed: 21613983]
78. Laurila K, Vihinen M. 2009. Prediction of disease-related mutations affecting protein localization. BMC Genom. 10:122

79. Paronetto MP. 2013. Ewing sarcoma protein: a key player in human cancer. Int. J. Cell Biol 2013:642853 [PubMed: 24082883]
80. Park H, Kim H, Hassebroek V, Azuma Y, Slawson C, Azuma M. 2020. Chromosomal localization of Ewing sarcoma EWSR1/FLI1 protein promotes the induction of aneuploidy. J. Biol. Chem 296:100164 [PubMed: 33293370]
81. Weaver BAA, Cleveland DW. 2005. Decoding the links between mitosis, cancer, and chemotherapy: the mitotic checkpoint, adaptation, and cell death. Cancer Cell 8(1):7–12 [PubMed: 16023594]
82. Lacoste J, Haghighi M, Haider S, Reno C, Lin Z-Y, et al. 2024. Pervasive mislocalization of pathogenic coding variants underlying human disorders. Cell 187(23):6725–41.e13 [PubMed: 39353438]
83. Cutting GR. 2015. Cystic fibrosis genetics: from molecular understanding to clinical application. Nat. Rev. Genet 16(1):45–56 [PubMed: 25404111]
84. Lukasiak A, Zajac M. 2021. The distribution and role of the CFTR protein in the intracellular compartments. Membranes 11(11):804 [PubMed: 34832033]
85. Rimessi A, Vitto VAM, Patergnani S, Pinton P. 2021. Update on calcium signaling in cystic fibrosis lung disease. Front. Pharmacol 12:581645 [PubMed: 33776759]
86. Lundberg E, Borner GHH. 2019. Spatial proteomics: a powerful discovery tool for cell biology. Nat. Rev. Mol. Cell Biol 20(5):285–302 [PubMed: 30659282]
87. Huang P, Gao W, Fu C, Tian R. 2023. Functional and clinical proteomic exploration of pancreatic cancer. Mol. Cell Proteom 22(7):100575
88. Dagogo-Jack I, Shaw AT. 2018. Tumour heterogeneity and resistance to cancer therapies. Nat. Rev. Clin. Oncol 15(2):81–94 [PubMed: 29115304]
89. Proietto M, Crippa M, Damiani C, Pasquale V, Sacco E, et al. 2023. Tumor heterogeneity: preclinical models, emerging technologies, and future applications. Front. Oncol 13:1164535 [PubMed: 37188201]
90. Ng J, Pan E, Johnston A, Ribera NT, Kersbergen A, et al. 2024. A multiplexed approach to assess small cell lung cancer subtype heterogeneity in primary and patient-derived tumor samples. Methods Mol. Biol 2806:117–38 [PubMed: 38676800]
91. Chou K-C, Cai Y-D. 2002. Using functional domain composition and support vector machines for prediction of protein subcellular location. J. Biol. Chem 277(48):45765–69 [PubMed: 12186861]
92. Almagro Armenteros JJ, Sønderby CK, Sønderby SK, Nielsen H, Winther O.2017. DeepLoc: prediction of protein subcellular localization using deep learning. Bioinformatics 33(21):3387–95 [PubMed: 29036616]
93. Pan X, Zeng T, Zhang Y-H, Chen L, Feng K, et al. 2020. Investigation and prediction of human interactome based on quantitative features. Front. Bioeng. Biotechnol 8:730 [PubMed: 32766217]
94. Goldberg T,Hamp T,Rost B.2012.LocTree2 predicts localization for all domains of life. Bioinformatics 28(18):i458–65 [PubMed: 22962467]
95. Schubert W, Bonnekoh B, Pommer AJ, Philipsen L, Böckelmann R, et al. 2006. Analyzing proteome topology and function by automated multidimensional fluorescence microscopy. Nat. Biotechnol 24(10):1270–78 [PubMed: 17013374]
96. Halabi EA, Weissleder R. 2023. Light-deactivated fluorescent probes (FLASH-Off) for multiplexed imaging. J. Am. Chem. Soc 145(15):8455–63
97. Tan WCC, Nerurkar SN, Cai HY, Ng HHM, Wu D, et al. 2020. Overview of multiplex immunohistochemistry/immunofluorescence techniques in the era of cancer immunotherapy. Cancer Commun. 40(4):135–53
98. Reiber T, Dose C, Yushchenko DA. 2024. A novel dual-release scaffold for fluorescent labels improves cyclic immunofluorescence. RSC Chem. Biol 5(7):684–90 [PubMed: 38966675]
99. Ko J, Oh J, Ahmed MS, Carlson JCT, Weissleder R. 2020. Ultra-fast cycling for multiplexed cellular fluorescence imaging. Angew. Chem. Int. Ed 59(17):6839–46
100. Ko J, Wilkovitsch M, Oh J, Kohler RH, Bolli E, et al. . 2022. Spatiotemporal multiplexed immunofluorescence imaging of living cells and tissues with bioorthogonal cycling of fluorescent probes. Nat. Biotechnol 40(11):1654–62 [PubMed: 35654978]

101. Wilkovitsch M, Haider M, Sohr B, Herrmann B, Klubnick J, et al. . 2020. A cleavable C_2-symmetric *trans*-cyclooctene enables fast and complete bioorthogonal disassembly of molecular probes. J.Am.Chem.Soc 142(45):19132–41 [PubMed: 33119297]
102. Carpenter AE, Jones TR, Lamprecht MR, Clarke C, Kang IH, et al. 2006. CellProfiler: image analysis software for identifying and quantifying cell phenotypes. Genome Biol. 7(10):R100 [PubMed: 17076895]
103. Chiu C-L, Clack N, the napari community. 2022. napari: a python multi-dimensional image viewer platform for the research community. Microsc. Microanal 28(Suppl. 1):1576–77
104. Berg S, Kutra D, Kroeger T, Straehle CN, Kausler BX, et al. 2019. ilastik: interactive machine learning for (bio)image analysis. Nat. Methods 16(12):1226–32 [PubMed: 31570887]
105. Jarosch S, Köhlen J, Sarker RSJ, Steiger K, Janssen K-P, et al. 2021. Multiplexed imaging and automated signal quantification in formalin-fixed paraffin-embedded tissues by ChipCytometry. Cell Rep. Methods 1(7):100104 [PubMed: 35475000]
106. Goltsev Y, Samusik N, Kennedy-Darling J, Bhate S, Hale M, et al. 2018. Deep profiling of mouse splenic architecture with CODEX multiplexed imaging. Cell 174(4):968–81.e15 [PubMed: 30078711]
107. Niemeyer CM, Adler M, Wacker R. 2007. Detecting antigens by quantitative immuno-PCR. Nat. Protoc 2(8):1918–30 [PubMed: 17703203]
108. Malou N, Raoult D. 2011. Immuno-PCR: a promising ultrasensitive diagnostic method to detect antigens and antibodies. Trends Microbiol. 19(6):295–302 [PubMed: 21478019]
109. Reynolds DE, Sun Y, Wang X, Vallapureddy P, Lim J, et al. 2024. Live organoid cyclic imaging. Adv. Sci 11(14):2309289
110. Bhaumik S, Boyer J, Banerjee C, Clark S, Sebastiao N, et al. 2020. Fluorescent multiplexing of 3D spheroids: analysis of biomarkers using automated immunohistochemistry staining platform and multispectral imaging. J. Cell. Biochem 121(12):4974–90 [PubMed: 32692912]
111. Dinevska M, Widodo SS, Mantamadiotis T. 2024. High-throughput multiplex immunohistochemistry of glioma organoids. In Neurobiology: Methods and Protocols, ed. Dworkin S, pp. 57–65. Springer
112. Harter MF, Recaldin T, Gerard R, Avignon B, Bollen Y, et al. 2024. Analysis of off-tumour toxicities of T-cell-engaging bispecific antibodies via donor-matched intestinal organoids and tumouroids. Nat. Biomed. Eng 8(4):345–60 [PubMed: 38114742]
113. Tomov ML, O'Neil A, Abbasi HS, Cimini BA, Carpenter AE, et al. 2021. Resolving cell state in iPSC-derived human neural samples with multiplexed fluorescence imaging. Commun. Biol 4(1):786 [PubMed: 34168275]
114. White SL, Lam AT, Buck HD. 2023. 3D imaging for cleared tissues and thicker samples on confocal and light-sheet microscopes. In Signal Transduction Immunohistochemistry: Methods and Protocols, ed. Kalyuzhny AE, pp. 143–61. Springer
115. Yoon S, Cheon SY, Park S, Lee D, Lee Y, et al. 2022. Recent advances in optical imaging through deep tissue: imaging probes and techniques. Biomater. Res 26(1):57 [PubMed: 36273205]
116. Flint LE, Hamm G, Ready JD, Ling S, Duckett CJ, et al. 2020. Characterization of an aggregated three-dimensional cell culture model by multimodal mass spectrometry imaging. Anal. Chem92(18):12538–47 [PubMed: 32786495]
117. Chang Q, Ornatsky OI, Siddiqui I, Loboda A, Baranov VI, Hedley DW. 2017. Imaging mass cytometry. Cytometry A 91(2):160–69 [PubMed: 28160444]
118. Flint L 2023. Multimodal mass spectrometry imaging of an aggregated 3D cell culture model. In Imaging Mass Spectrometry: Methods and Protocols, ed. Cole LM, Clench MR, pp. 147–59. Springer
119. Baars MJD, Sinha N, Amini M, Pieterman-Bos A, van Dam S, et al. 2021. MATISSE: a method for improved single cell segmentation in imaging mass cytometry. BMC Biol. 19(1):99 [PubMed: 33975602]
120. Giesen C, Wang HAO, Schapiro D, Zivanovic N, Jacobs A, et al. 2014. Highly multiplexed imaging of tumor tissues with subcellular resolution by mass cytometry. Nat. Methods 11(4):417–22 [PubMed: 24584193]

121. Angelo M, Bendall SC, Finck R, Hale MB, Hitzman C, et al. 2014. Multiplexed ion beam imaging of human breast tumors. Nat. Med 20(4):436–42 [PubMed: 24584119]
122. Keren L, Bosse M, Thompson S, Risom T, Vijayaragavan K, et al. 2019. MIBI-TOF: a multiplexed imaging platform relates cellular phenotypes and tissue structure. Sci. Adv 5(10):eaax5851 [PubMed: 31633026]
123. Greenwald NF, Miller G, Moen E, Kong A, Kagel A, et al. 2022. Whole-cell segmentation of tissue images with human-level performance using large-scale data annotation and deep learning. Nat. Biotechnol 40(4):555–65 [PubMed: 34795433]
124. Baharlou H, Canete NP, Cunningham AL, Harman AN, Patrick E. 2019. Mass cytometry imaging for the study of human diseases—applications and data analysis strategies. Front. Immunol 10:2657 [PubMed: 31798587]
125. Risom T, Chang P, Rost S, Ziai J. 2023. Mass spectrometry–based tissue imaging of the tumor microenvironment. In Cancer Systems and Integrative Biology, ed. Kasid UN, Clarke R, pp. 171–85. Springer
126. Hickey JW, Tan Y, Nolan GP, Goltsev Y. 2021. Strategies for accurate cell type identification in CODEX multiplexed imaging data. Front. Immunol 12:727626 [PubMed: 34484237]
127. Hosogane T, Casanova R, Bodenmiller B. 2023. DNA-barcoded signal amplification for imaging mass cytometry enables sensitive and highly multiplexed tissue imaging. Nat. Methods 20(9):1304–9 [PubMed: 37653118]
128. Deng K, Zhan L, Yi L, Zhang J, Tang M, et al. 2025. Deepening imaging-based spatial proteomics at high spatial resolution through controlled tissue resizing and in-situ bottom-up mass spectrometry. Preprint, bioRxiv. https://www.biorxiv.org/content/10.1101/2025.06.12.659329v1
129. Li L, Sun C, Sun Y, Dong Z, Wu R, et al. 2022. Spatially resolved proteomics via tissue expansion. Nat. Commun 13:7242 [PubMed: 36450705]
130. Rae Buchberger A, DeLaney K, Johnson J, Li L. 2018. Mass spectrometry imaging: a review of emerging advancements and future insights. Anal. Chem 90(1):240–65 [PubMed: 29155564]
131. Zhang H, Delafield DG, Li L. 2023. Mass spectrometry imaging: the rise of spatially resolved single-cell omics. Nat. Methods 20(3):327–30 [PubMed: 36899158]
132. Bergman H-M, Lundin E, Andersson M, Lanekoff I. 2016. Quantitative mass spectrometry imaging of small-molecule neurotransmitters in rat brain tissue sections using nanospray desorption electrospray ionization. Analyst 141(12):3686–95 [PubMed: 26859000]
133. Caldwell RL, Caprioli RM. 2005. Tissue profiling by mass spectrometry: a review of methodology and applications. Mol. Cell. Proteom 4(4):394–401
134. Iqfath M, Wali SN, Amer S, Hernly E, Laskin J. 2024. Nanospray desorption electrospray ionization mass spectrometry imaging (nano-DESI MSI): a tutorial review. ACS Meas. Sci. Au 4(5):475–87 [PubMed: 39430971]
135. Lanekoff I, Laskin J. 2015. Imaging of lipids and metabolites using nanospray desorption electrospray ionization mass spectrometry. In Mass Spectrometry Imaging of Small Molecules, ed. He L, pp. 99–106. Springer
136. Yang M, Unsihuay D, Hu H, Meke FN, Qu Z, et al. 2023. Nano-DESI mass spectrometry imaging of proteoforms in biological tissues with high spatial resolution. Anal. Chem 95(12):5214–22 [PubMed: 36917636]
137. Bhatia HS, Brunner A-D, Öztürk F, Kapoor S, Rong Z, et al. 2022. Spatial proteomics in three-dimensional intact specimens. Cell 185(26):5040–58.e19 [PubMed: 36563667]
138. Doerr A 2023. DISCO-MS combines spatial proteomics with whole-organ imaging. Nat. Biotechnol 41(2):194
139. Zhang H, Ding L, Hu A, Shi X, Huang P, et al. 2025. TEMI: tissue-expansion mass-spectrometry imaging. Nat. Methods 22(5):1051–58 [PubMed: 40263584]
140. Xu Y, Lih TM, De Marzo AM, Li QK, Zhang H. 2024. SPOT: spatial proteomics through on-site tissue-protein-labeling. Clin. Proteom 21:60
141. Mund A, Coscia F, Kriston A, Hollandi R, Kovács F, et al. 2022. Deep Visual Proteomics defines single-cell identity and heterogeneity. Nat. Biotechnol 40(8):1231–40 [PubMed: 35590073]

142. Rosenberger FA, Mädler SC, Thorhauge KH, Steigerwald S, Fromme M, et al. 2025. Deep Visual Proteomics maps proteotoxicity in a genetic liver disease. Nature 642:484–91 [PubMed: 40240610]

143. Zheng X, Pedersen LM, Bzorek M, Mund A, Gjerdrum LMR, Mann M. 2024. Deep Visual Proteomics unveils precision medicine insights in composite small lymphocytic and classical Hodgkin lymphoma. Preprint, bioRxiv. https://www.biorxiv.org/content/10.1101/2024.06.12.598635v1

144. Espina V, Wulfkuhle JD, Calvert VS, VanMeter A, Zhou W, et al. 2006. Laser-capture microdissection. Nat. Protoc 1(2):586–603 [PubMed: 17406286]

145. Zheng X, Mund A, Mann M. 2025. Deciphering functional tumor-immune crosstalk through highly multiplexed imaging and deep visual proteomics. Mol. Cell 85(5):1008–23.e7 [PubMed: 39814024]

146. Qin R, Ma J, He F, Qin W. 2025. In-depth and high-throughput spatial proteomics for whole-tissue slice profiling by deep learning-facilitated sparse sampling strategy. Cell Discov. 11(1):21 [PubMed: 40064869]

147. Hu B, He R, Pang K, Wang G, Wang N, et al. 2025. High-resolution spatially resolved proteomics of complex tissues based on microfluidics and transfer learning. Cell 188(3):734–48.e22 [PubMed: 39855194]

148. Larsen MR, Edwards AVG. 2016. Phosphoproteomics: approaches, developments, and challenges. In Encyclopedia of Cell Biology, ed. Bradshaw RA, Stahl PD, pp. 177–86. Academic

149. Hu B, Zhu J, Zhao F. 2024. The evolving landscape of spatial proteomics technologies in the AI age. Fundam. Res 6:28–39 [PubMed: 41647570]

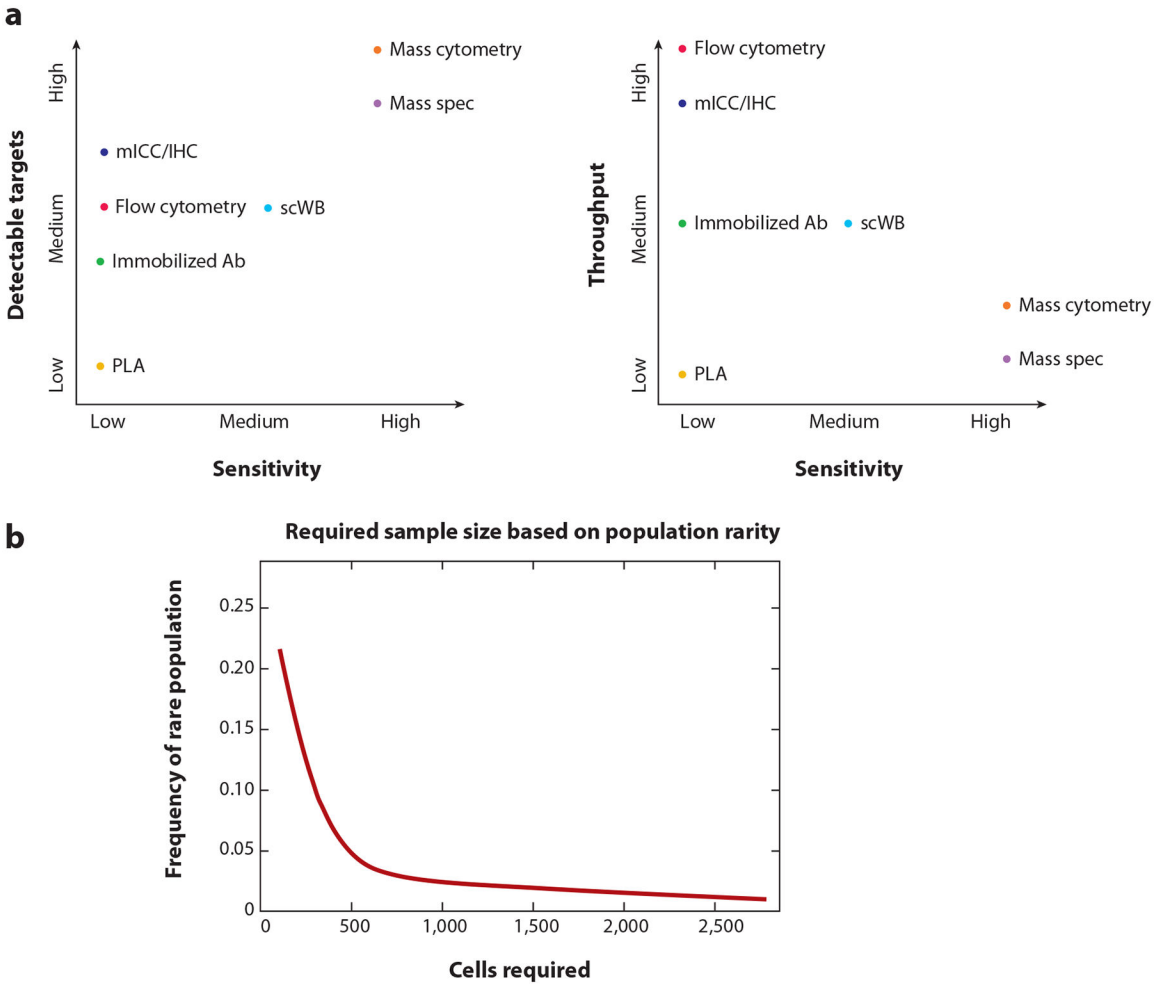

Figure 1.

Considerations for choosing a scP technique. (*a*) scP technique sensitivity compared to throughput and multiplexing capabilities. Panel *a* adapted with permission from Reference 8; copyright 2018 Essays in Biochemistry. (*b*) Number of cells from a heterogeneous population needed for analysis to gain a 0.95 probability of sequencing 20 cells from a rare subpopulation. Plot data generated with SCOPIT (7). Abbreviations: Ab, antibody; IHC, immunohistochemistry; Mass spec, mass spectrometry; mICC, multiplexed immunocytochemistry; PLA, proximity-ligation assay; scP, single-cell proteomics; scWB, single-cell western blot. Figure adapted from images created in BioRender. Baker, J., Joseph, N., Lao, A., Vlassakis, J. 2025. https://BioRender.com/xp4b2zz.

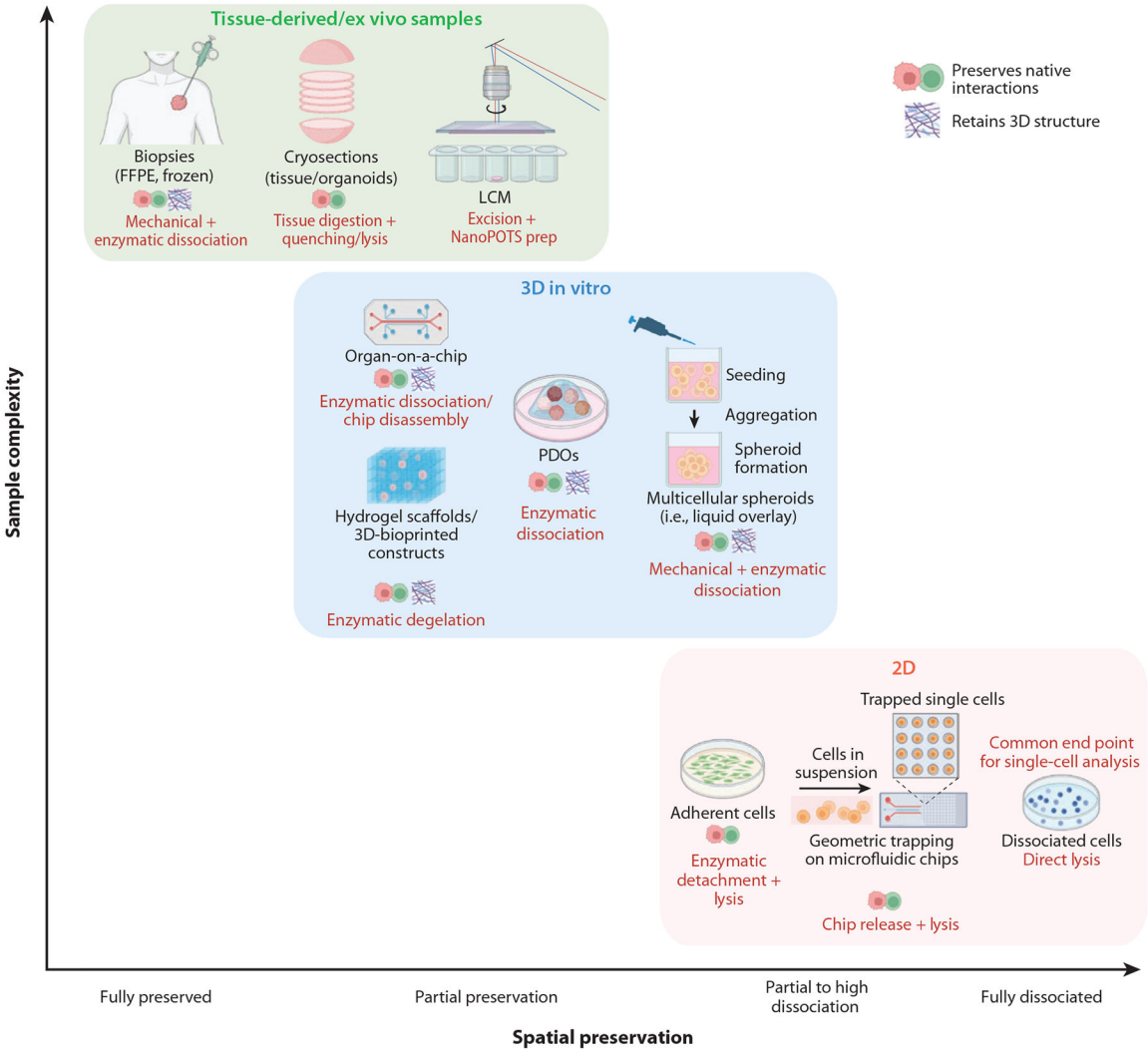

Figure 2.

Sample models arranged by spatial dissociation and biological complexity. This framework highlights trade-offs between spatial context and accessibility for single-cell analysis. Abbreviations: 2D, two dimensional; 3D, three dimensional; FFPE, formalin-fixed paraffin-embedded; LCM, laser capture microdissection; nanoPOTS, nanodroplet processing in one pot for trace samples; PDO, patient-derived organoid. Figure adapted from images created in BioRender. Baker, J., Joseph, N., Lao, A., Vlassakis, J. 2025. https://BioRender.com/jp4mr51.

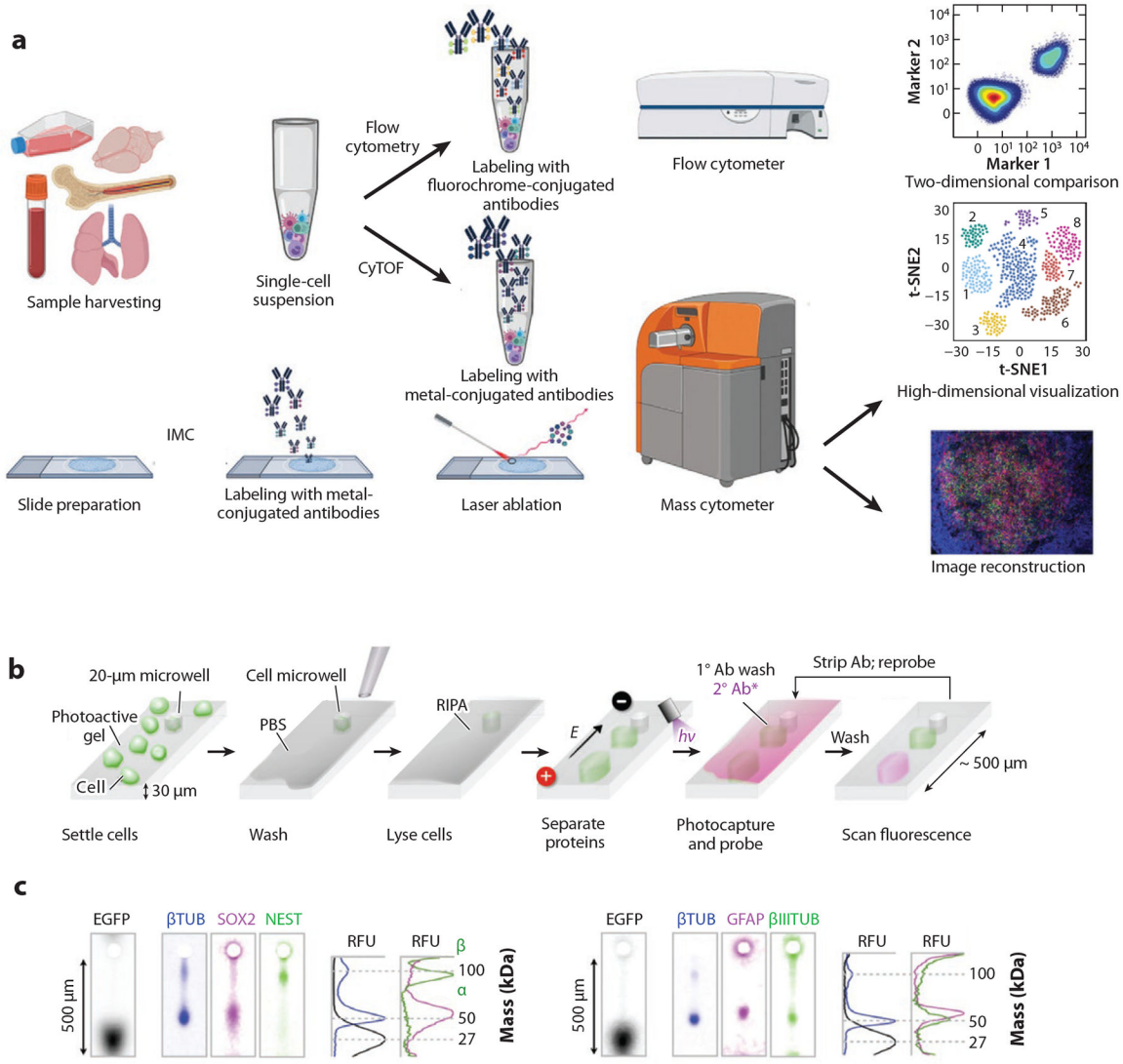

Figure 3.

Single-cell cytometry and immunoblotting techniques. (*a*) CyTOF workflow for dissociated and laser-ablated samples. (*b*) scWB technique workflow. (*c*) False-colored fluorescence micrographs and intensity profiles from scWBs of neural stem cells to identify protein isoform expression at two different timepoints in differentiation. Panel *a* adapted with permission from Reference 34; copyright 2021 John Wiley & Sons. Panels *b* and *c* adapted with permission from Reference 35; copyright 2014 Springer Nature. Abbreviations: βTUB, beta-tubulin; Ab, antibody; CyTOF, cytometry by time of flight; EGFP, enhanced green fluorescent protein; GFAP, glial fibrillary acidic protein; *hv*, photon energy; IMC, imaging mass cytometry; NEST, nestin; PBS, phosphate-buffered saline; RFU, relative fluorescence unit; RIPA, radioimmunoprecipitation assay buffer; scWB, single-cell western blotting; SOX2, sex determining region Y-box transcription factor 2; t-SNE, t-distributed stochastic neighbor embedding.

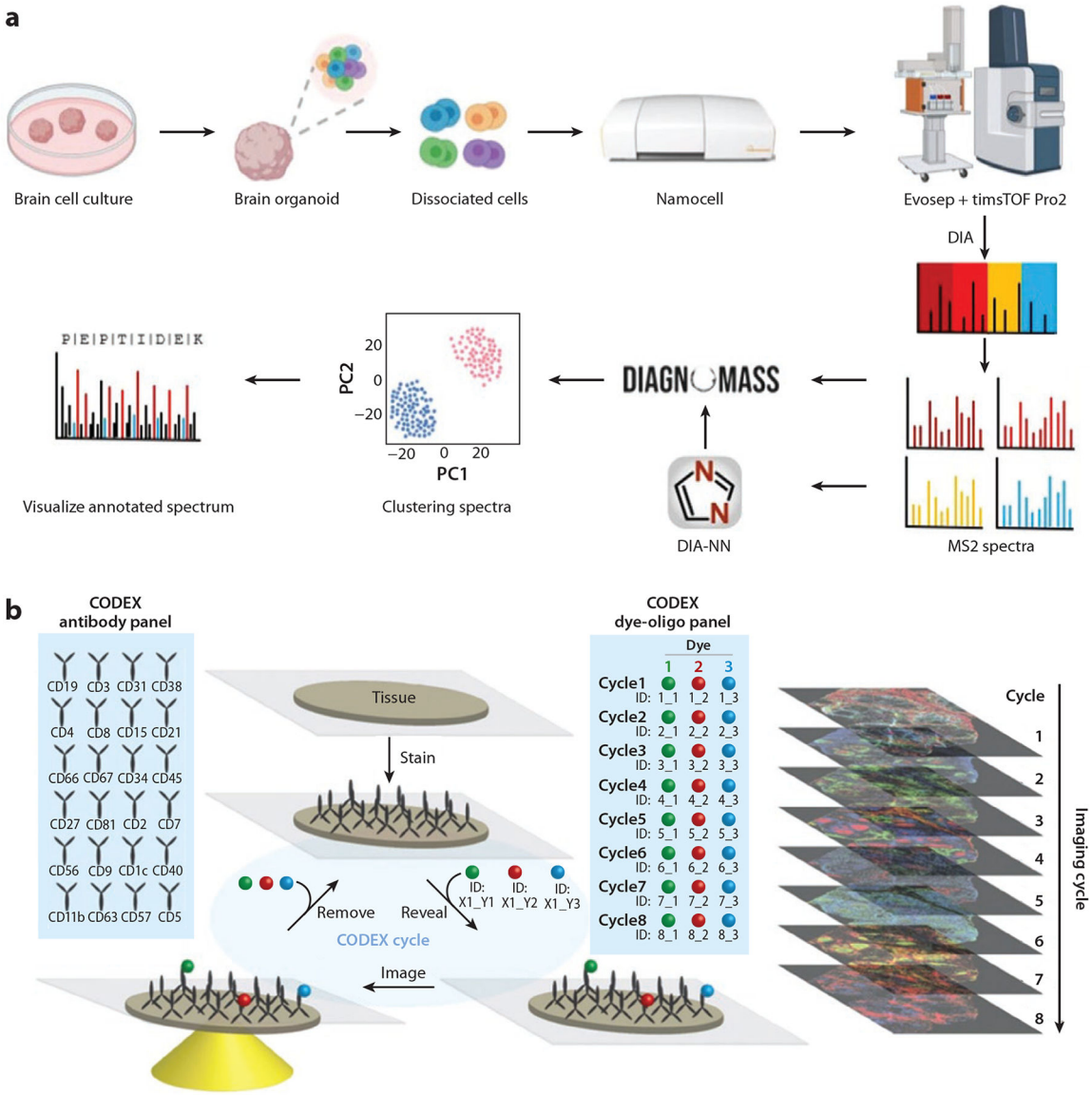

Figure 4.

Single-cell multiplexed ICC and MS techniques. (*a*) DIA single-cell workflow. Panel *a* adapted with permission from Reference 68; copyright 2024 American Chemical Society. (*b*) CODEX workflow for analyzing single-cell protein expression in tissues. Panel *b* adapted with permission from Reference 61; copyright 2021 John Wiley & Sons. Abbreviations: CODEX, co-detection by indexing; DIA, data-independent acquisition; ICC, immunocytochemistry; MS, mass spectrometry; timsTOF, trapped ion mobility spectrometry time of flight.

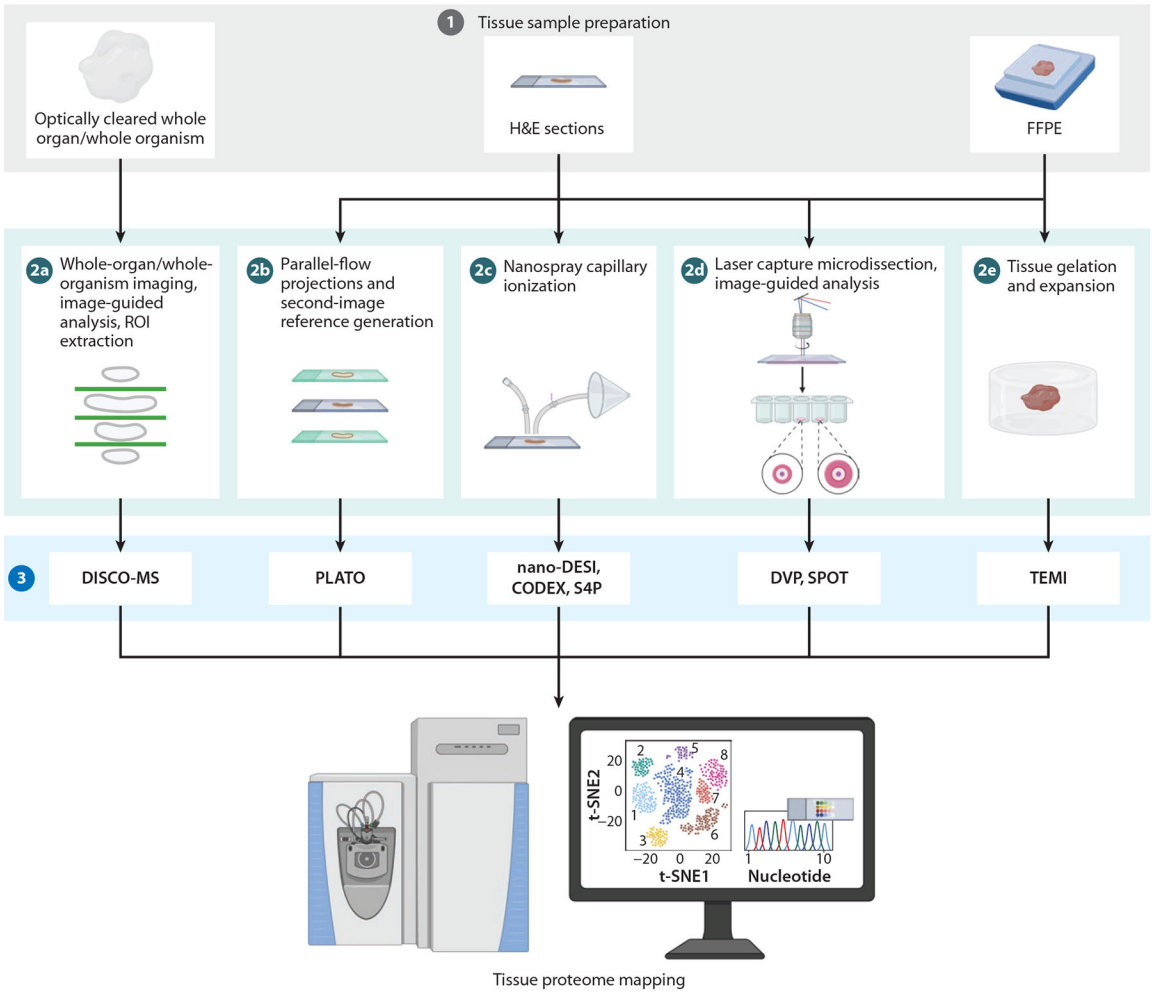

Figure 5.

In situ spatial proteomics approaches. A flow chart highlighting some similarities and differences between MS-based (DISCO-MS, nano-DESI, SPOT, TEMI) and intelligent image–based (PLATO, CODEX, DVP, S4P) approaches. (①) Typical tissue sample type. (②, *a*–*e*) Defining steps of MS- or intelligent image–based techniques. (③) In situ spatial proteomics technique name. Abbreviations: CODEX, co-detection by indexing; DISCO-MS, 3D imaging of solvent-cleared organs profiled by mass spectrometry; DVP, deep visual proteomics; FFPE, formalin-fixed paraffin-embedded; H&E, hematoxylin and eosin; MS, mass spectrometry; nano-DESI, nanospray desorption electrospray ionization; PLATO, parallel-flow projection and transfer learning across omics data; ROI, region of interest; S4P, sparse sampling strategy for spatial proteomics; SPOT, spatial proteomics through on-site tissue protein labeling; TEMI, tissue expansion mass spectrometry imaging; t-SNE, t-distributed stochastic neighbor embedding. Figure adapted from images created in BioRender. Baker, J., Joseph, N., Lao, A., Vlassakis, J. 2025. https://BioRender.com/a1sdq9w.

Table 1

Benchmarking table comparing various scP methods

scP method	Spatial preservation[a]	Protein targets detectable	Cells required/ assay (minimum)	Cell throughput/ assay	Selectivity	Cost[b]
Proximity-ligation assay	Yes (tissue samples)	~22 (5), 3 in situ (11)	Tens of thousands	Hundreds	Immunoaffinity	$
Immobilized antibody	No	16 (12–14)	Hundreds	Hundreds to thousands	Immunoaffinity	$
Single-cell capillary electrophoresis	No	Hundreds to thousands (MS paired) (15)	Dozens	Tens	Immunoaffinity and protein sizing	$–$$$
Flow cytometry	No	30 (16)	Thousands	Tens of thousands	Immunoaffinity	$
Single-cell western blot	No	~25 (17)	Hundreds	Thousands	Immunoaffinity and protein sizing	$
Multiplexed IHC/ICC	Yes	Tens	Thousands	Tens of thousands	Immunoaffinity or mass-to-charge ratio	$$–$$$
Mass cytometry	No	Tens (18, 19)	Dozens	Tens of thousands	Immunoaffinity	$$$
MS	Yes in some cases	Hundreds (20–22)	Dozens	Tens	Mass-to-charge ratio	$$$

[a]Preservation of spatial information/structures such as cell localization in tissues, cell–cell connections, and cell morphology.

[b]The dollar signs (from one to three) denote relative costs, taking into account cost of equipment and materials.

Abbreviations: ICC, immunocytochemistry; IHC, immunohistochemistry; MS, mass spectrometry; scP, single-cell proteomics.